Journal of Solid State Chemistry 184 (2011) 1361–1366

Contents lists available at ScienceDirect

Journal of Solid State Chemistry

journal homepage: www.elsevier.com/locate/jssc

Structure and magnetic properties of the cubic oxide fluoride $BaFeO_2F$

Frank J. Berry [a,b,*], Fiona C. Coomer [a], Cathryn Hancock [a], Örn Helgason [c], Elaine A. Moore [b], Peter R. Slater [a], Adrian J. Wright [a], Michael F. Thomas [d]

[a] School of Chemistry, The University of Birmingham, Edgbaston, Birmingham B15 2TT, UK
[b] Department of Chemistry, The Open University, Walton Hall, Milton Keynes MK7 6AA, UK
[c] Science Institute, University of Iceland, Dunhagi 3, IS-107 Reykjavik, Iceland
[d] Department of Physics, The University of Liverpool, Liverpool L69 3BX, UK

ARTICLE INFO

Article history:
Received 8 November 2010
Received in revised form
3 March 2011
Accepted 4 April 2011
Available online 14 April 2011

Keywords:
$BaFeO_2F$
Oxide fluoride
Canted antiferromagnet

ABSTRACT

Fluorination of the parent oxide, $BaFeO_{3-\delta}$, with polyvinylidine fluoride gives rise to a cubic compound with $a=4.0603(4)$ Å at 298 K. ^{57}Fe Mössbauer spectra confirmed that all the iron is present as Fe^{3+}. Neutron diffraction data showed complete occupancy of the anion sites, indicating a composition $BaFeO_2F$, with a large displacement of the iron off-site. The magnetic ordering temperature was determined as $T_N=645\pm5$ K. Neutron diffraction data at 4.2 K established G-type antiferromagnetism with a magnetic moment per Fe^{3+} ion of 3.95 μ_B. However, magnetisation measurements indicated the presence of a weak ferromagnetic moment that is assigned to the canting of the antiferromagnetic structure. ^{57}Fe Mössbauer spectra in the temperature range 10–300 K were fitted with a model of fluoride ion distribution that retains charge neutrality of the perovskite unit cell.

1. Introduction

The identification of superconductivity in oxide fluorides of composition $Sr_2CuO_2F_{2+x}$, which adopt a perovskite-related structure, has generated considerable activity in the synthesis and characterisation of new inorganic oxide fluorides with related structures [1–3]. We have recently reported [4,5] on the fluorination of oxygen-deficient perovskite-related $SrFeO_{3-\delta}$ to give a compound of composition $SrFeO_2F$ with a cubic unit cell and have formulated a model related to the pattern of substitution by fluorine on the octahedral arrangement of oxygen sites around iron in which $SrFeO_2F$ undergoes a magnetic transition around 300 K from a low temperature state with random spin directions to an antiferromagnetic state. We have also prepared the related cubic phase of composition $BaFeO_2F$ and, in a preliminary neutron powder diffraction study, found it to exhibit G-type antiferromagnetic order at 298 K [6]. However, this preliminary study [6] generated significant questions that required further detailed investigation. For example, the high thermal displacement parameter (3.6 Å^2) for the iron site suggests the possibility of a series of random displacements. However, the fact that the sample possesses cubic symmetry implies that if such displacements are present there is no unique direction for them, which raises the question of whether, at lower temperatures, a phase transition to a non-centrosymmetric ferroelectric cell may occur leading to the co-existence of magnetic- and ferroelectric-order. In order to address these matters we have recorded neutron powder diffraction data at 4.2 K and, in order to investigate further the magnetic properties of the material, we have recorded DC susceptibility measurements between 5 and 300 K and field-dependent DC measurements at 5 K between 0 and 7 T together with Mössbauer spectra between 300 and 10 K. We have also performed calculations to explore the displacement of iron and magnetic interactions within the material.

Hence we now report here on an examination of the structural and magnetic properties of cubic $BaFeO_2F$ between 4.2 and 650 K, which modifies the preliminary description of the material [6] and shows it to be substantially different from $SrFeO_2F$.

2. Experimental

The oxygen deficient $BaFeO_{3-\delta}$ was prepared by the calcination of appropriate quantities of a well ground mixture of barium(II) carbonate and iron(III) oxide at 1100 °C for 24 h in air with intermediate regrinding. Fluorination was achieved by mixing the $BaFeO_{3-\delta}$ phase with polyvinylidene fluoride in a 1:0.60 molar ratio (precursor oxide:monomer unit) [7] and heating this mixture at 375 °C for 24 h in air in a furnace within a fume cupboard.

* Corresponding author at: School of Chemistry, The University of Birmingham, Edgbaston, Birmingham B15 2TT, UK.
E-mail address: f.j.berry.1@bham.ac.uk (F.J. Berry).

0022-4596/$ - see front matter © 2011 Elsevier Inc. All rights reserved.
doi:10.1016/j.jssc.2011.04.011

X-ray powder diffraction patterns were recorded with a Panalytical X′ Pert Pro diffractometer using Cu$K\alpha$ radiation at 298 K. Neutron diffraction data were collected at 4.2 K on the POLARIS diffractometer, ISIS, Rutherford Appleton Laboratory. All structure refinements used the GSAS suite of the Rietveld refinement software [8].

DC susceptibility measurements were performed over the temperature range 5–300 K using a Quantum Design MPMS SQUID magnetometer. The samples were pre-cooled to 5 K in zero field (ZFC) and also in an applied field of 0.1 T (FC) and values of χ measured whilst warming in a field of 0.1 T. Field-dependent DC susceptibility measurements were performed with a Quantum Design PPMS system with the ACMS control system in DC extraction mode. Measurements were performed at 5 K between 0 and 7 T.

The ^{57}Fe Mössbauer spectra were recorded between 10 and 650 K with a constant acceleration spectrometer using a Co/Rh source of ca. 25 mCi. The spectra between 10 and 300 K were recorded with a liquid helium flow cryostat and spectra between 400 and 650 K were recorded *in situ* using a specially designed furnace [9]. The ^{57}Fe Mössbauer chemical isomer shift data are quoted relative to metallic iron at room temperature.

Calculations were performed using CRYSTAL06 [10] on $2\times2\times2$ supercells of cubic $BaFeO_2F$ using the experimental cell dimensions. Such a supercell permits exploration of the different types of antiferromagnetism. The basis sets used were all electron sets on Fe{8-6411-d41} [11], O{8-411-d1} [12] and F{7-311} [13]. A pseudopotential basis set [14] was used for Ba to reduce the computer resource needed. The hybrid functional B3LYP was used as it has been shown that methods beyond DFT such as hybrid functionals and DFT+U are needed for the correct description of solids with highly correlated cations. Supercells with the iron ions surrounded by four oxide and two fluoride ions with the fluoride ions arranged trans or cis were used. Ferromagnetic and A-, C- and G-type antiferromagnetic spin arrangements were explored for the lowest energy configuration.

3. Results and discussion

3.1. X-ray and neutron powder diffraction

The X-ray powder diffraction pattern recorded from $BaFeO_2F$ at 298 K indicated a cubic phase with unit cell size, $a=4.0603(4)$ Å. The structure of this phase was previously examined by neutron diffraction at 298 and 773 K [6] and confirmed cubic symmetry and indicated G-type antiferromagnetic order at the former temperature. However, as noted earlier, the work suggested some displacement of the iron [6]. In an extension of this work, we have now analysed the structure at low temperature (4.2 K) to determine if there is a lowering of symmetry and hence a phase transition to a non-centrosymmetric unit cell. The low temperature data showed very little change from the room temperature data, with a cubic cell and magnetic (G-type antiferromagnet) ordering. Calculations supported the G-type antiferromagnetic cell as the lowest energy ordering at low temperature if spin–orbit coupling is neglected. The refined structural parameters are given in Table 1 with selected bond distances in Table 2, and the neutron diffraction profiles are shown in Fig. 1. The results show that, as in the case of the room temperature data, there remains a high thermal displacement parameter for the iron, indicating some off centre displacement. The fact that the cell symmetry is cubic means that there is no unique long range direction for these displacements. Instead there are likely to be local displacements that may be influenced by both the large size of barium, which leads to underbonding at the B cation site and the mixed occupation of anion sites by F^- and O^{2-} ions. To illustrate the underbonding at the iron site, bond valence calculations showed that for a Fe(III)O_4F_2 octahedron, the bond valence sum (BVS) is 2.76.

Table 1
Refined structural parameters for $BaFeO_2F$ at 4.2 K (no Fe displacement).

Atom	Site	x	y	z	$U_1(\times100)$ (Å^2)	Site occupancy
Ba	1*a*	0	0	0	0.08 (1)	1
Fe	1*b*	0.5	0.5	0.5	2.99 (2)	1
O/F	3*c*	0.5	0.5	0	0.461 (8)	1

Pm-3m, $a=4.0447(1)$ Å, Chi$^2=3.16$, $R_{wp}=0.0138$, $R_p=0.0222$, Fe magnetic moment= 3.94(4) μ_B

Table 2
Selected bond distances for $BaFeO_2F$ at 4.2 K (no Fe displacement).

Bond	Bond distance (Å)
Fe–O/F	2.0224 (1) ($\times6$)
Ba–O/F	2.8601 (1) ($\times12$)

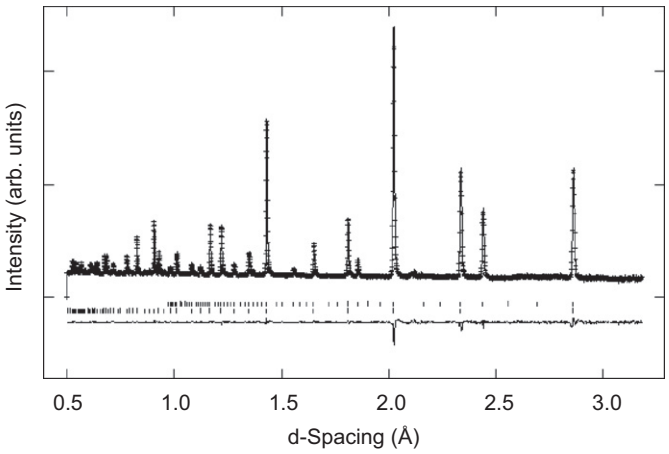

Fig. 1. Observed, calculated and difference neutron powder diffraction profiles for $BaFeO_2F$ at 4.2 K (the lower tick marks are the crystallographic structure reflections; the upper tick marks are the magnetic structure reflections).

The potential effect of the O/F distribution can be considered as follows. The charge neutral perovskite unit cell contains four O^{2-} and two F^- ions. Random occupation of the six anion sites gives cis or trans configurations in a ratio of 4:1. The Coulomb attraction between O^{2-} and Fe^{3+} ions is twice that between F^- and Fe^{3+} ions because of the double negative charge on the O^{2-} ion. However, the core size of the F^- ion will be less than that of the O^{2-} ion because of the greater nuclear charge, 9(F) as opposed to 8(O). In ionic bonding these Coulomb attraction and core repulsion terms act in opposition. While detailed calculations would be required to determine quantitatively the net effect it is easily appreciated that the ionic bonding along a line O^{2-}–Fe^{3+}–F^- should be unbalanced leading to a displacement of the Fe^{3+} ion. In the trans configuration there would be predicted to be no net displacement of the Fe^{3+} ion as in all directions the opposite forces are balanced but in the cis configuration displacements of the Fe^{3+} ion will be predicted to occur. An indication of the effect of O^{2-},F^- distribution on iron displacement is provided by periodic ab initio calculations on a structure in which all Fe^{3+} ions adopt the cis configuration. Optimisation of the atomic positions within the cell leads to a displacement of the Fe^{3+} ion towards the O^{2-} ions trans to the F^-. The calculations suggest displacement along the F–Fe–F angle bisector with Fe–O distances

Table 3
Refined structural parameters for $BaFeO_2F$ at 4.2 K (with Fe displacement).

Atom	Site	x	y	z	$U_1(\times 100)$ (Å^2)	Site occupancy
Ba	1*a*	0	0	0	0.08 (1)	1
Fe	6*e*	0.4386(3)	0.5	0.5	0.38 (3)	0.167
O/F	3*c*	0.5	0.5	0	0.464 (7)	1

Pm-3m, a=4.0447(1) Å, Chi^2=2.79, R_{wp}=0.0130, R_p=0.0224, Fe magnetic moment=3.99(4) μ_B.

Table 4
Selected bond distances for $BaFeO_2F$ at 4.2 K (with Fe displacement).

Bond	Bond distance (Å)
Fe–O/F	2.0376 (2) (× 4)
Fe–O/F	1.774 (1) (× 1)
Fe–O/F	2.271 (1) (× 1)
Ba–O/F	2.8601 (1) (× 12)

of 1.91 Å (for O^{2-} opposite F^-) and 2.05 Å and a Fe–F distance of 2.17 Å. If the F^- ions are randomly distributed (consistent with the neutral cell) the calculations would suggest that Fe^{3+} displacement will occur along all possible directions of these bisectors.

In order to investigate experimentally the direction of the displacements, the neutron diffraction data were re-examined and the iron allowed to move off-site. Interestingly, rather than a displacement along the bond angle bisector, a different displacement direction was observed with the experimental data being best fitted by moving the iron off the ideal 1*b* (1/2, 1/2, 1/2) site to the 6*f* (× , 1/2, 1/2) site with 1/6 occupancy. This refinement gave a stable position at (0.4386(3), 1/2, 1/2) with the atomic displacement parameter ($U_1(\times 100)$) reducing to 0.38 Å^2 and with a small improvement in the fit (Tables 3 and 4). This refinement therefore suggests an average shift of the iron off-site of ca. 0.25 Å directly along the Fe–O/F bond axis. Such a displacement is typical of ferroelectric-type displacements observed in perovskites such as $BaTiO_3$ and would suggest that local ferroelectric-type displacements are dominant as opposed to the effect of the local distribution of O/F examined by the modelling studies. The origin for this displacement is the large size of Ba leading to underbonding at the iron site, as highlighted above.

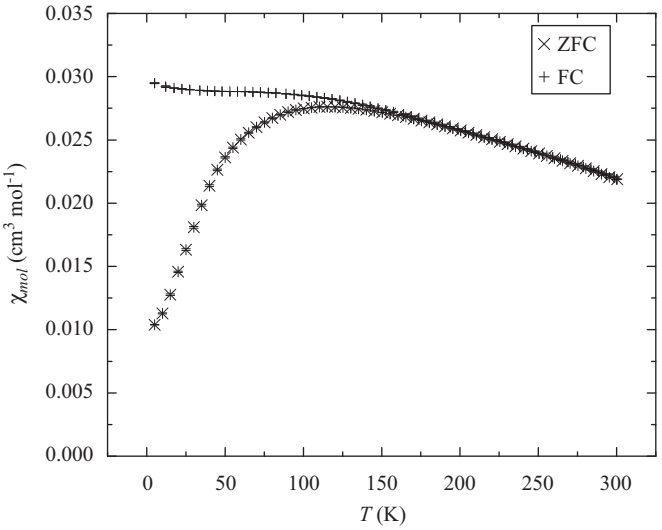

Fig. 2. Variation of magnetisation between 5 and 300 K. The data were recorded at increasing temperature in a measuring field of 0.1 T. Separate plots show field cooled (FC) and zero field cooled (ZFC) data.

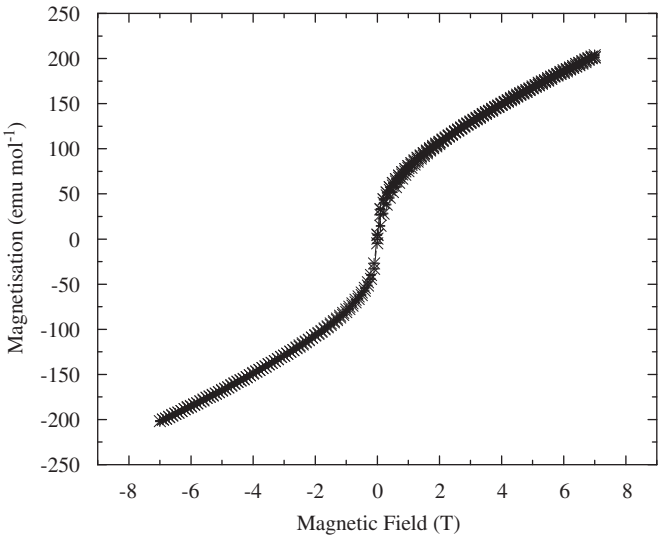

Fig. 3. Field dependent magnetisation measured at 5 K.

3.2. Magnetisation

The variation of magnetic susceptibility χ (in an applied field of 0.1 T) with increase in temperature from 5 to 300 K following pre-cooling in (i) zero applied field (ZFC) and (ii) an applied field of 0.1 T (FC) is shown in Fig. 2.

It is evident for $T<150$ K that there is a divergence in susceptibility data between zero field cooled (ZFC) samples and those cooled in an applied field of 0.1 T (FC). At temperatures above 150 K the data coincide and show a gentle decrease with increase in temperature. This behaviour modifies the picture of a pure G-type antiferromagnetic structure by indicating a weak ferromagnetic component.

The variation of magnetisation M in a field sweep measurement at 5 K is shown in Fig. 3.

It is seen that an increase in $|H|$ causes a relatively rapid increase in $|M|$ up to a value of $H\sim 0.2$ T whereupon there is a change of slope to one proportional to the increasing H. The shape of this M vs. H plot is characteristic of weak ferromagnetism where the steep initial slope arises from the saturation of the weak ferromagnetic component.

The magnitude of the weak moment was estimated by extrapolating a linear fit of the data in the range $4.5\ \text{T} \le H \le 7\ \text{T}$ to 0 T and measuring the intercept on the M-axis. This results in a value of $M=80\pm 1$ emu mol^{-1} equivalent to a moment per Fe^{3+} ion of 0.01 μ_B. Comparing this value with the Fe^{3+} moment of 3.95 μ_B equates to a canting angle, estimated by trigonometry from $\sin^{-1}(0.01/3.95)$, of $0.16\pm 0.02^\circ$.

3.2.1. Magnetisation results—the case for a weak ferromagnet

Neutron diffraction confirms that the basic magnetic structure of the Fe^{3+} moments is of a G-type antiferromagnet, but features of the susceptibility (χ) vs. temperature (T) plot (Fig. 2), particularly the divergence between ZFC and FC below ca. 150 K, suggest that a more complex description is necessary. Considering the presence of canting of the antiferromagnetic moments below ca. 150 K, it is possible to reconcile the appearance of the

susceptibility data with the neutron diffraction-determined magnetic structure. From the hysteresis data in Fig. 3 the magnitude of the weak ferromagnetic moment at 5 K has been evaluated as 0.01 μB per Fe^{3+} ion, suggesting a small canting angle of $0.16 \pm 0.02^{\circ}$, which would not be discernible *via* neutron diffraction.

Although we cannot exclude the possibility of the presence of separate magnetic impurities below the limit of detectability of the techniques used here we contend that the results, taken together and including the apparent continuous nature of the susceptibility data, supports our above interpretation in terms of a canted structure for the oxide fluoride.

3.3. *Mössbauer spectroscopy*

The ^{57}Fe Mössbauer spectra recorded between 10 and 300 K are shown in Fig. 4 and those recorded between 400 and 650 K are collected in Fig. 5. Representative ^{57}Fe Mössbauer parameters from Figs. 4 and 5 are collected in Table 5.

There are two features of the results presented in Figs. 4 and 5 and in Table 5, which are readily amenable to interpretation. Firstly, all the spectral components have chemical isomer shifts characteristic of the presence of Fe^{3+} ions which, together with the presence of Ba^{2+}, O^{2-} and F^{-} and the neutron diffraction data showing complete occupancy of the anion sites, is consistent with the formulation $BaFeO_2F$. Secondly, the spectra recorded at temperatures exceeding 400 K in Fig. 5 show decreasing magnitudes of magnetic hyperfine field until, at 650 K, the magnetic hyperfine field collapses to a quadrupole split doublet indicative of the paramagnetic state. The variation of the average magnetic hyperfine field with increase in temperature is shown in Fig. 6 and, from these data, a magnetic ordering temperature for $BaFeO_2F$ of 645 ± 5 K can be deduced. This is lower than the magnetic ordering temperature of 685 ± 5 K that was previously found for $SrFeO_2F$ [5]. The variation of the average magnetic hyperfine field with increase in temperature is also compared in Fig. 6 with that calculated from the expression $B = B_0(1 - T/T_c)^{\beta}$, where B is the magnetic hyperfine field and B_0 is the magnetic

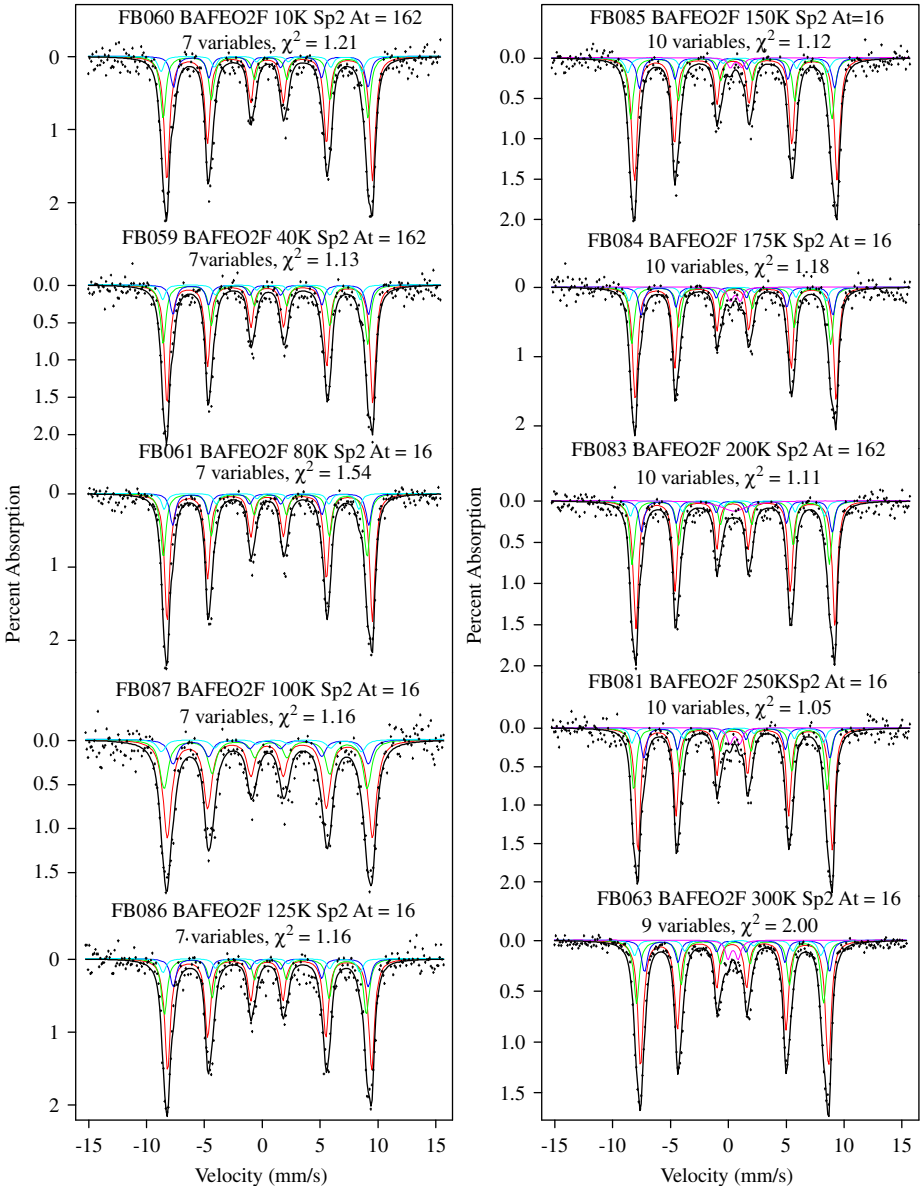

Fig. 4. ^{57}Fe Mössbauer spectra recorded from $BaFeO_2F$ between 10 and 300 K. The spectra were fitted with components constrained by a model of F^{-} distribution in which the unit perovskite cell contains four O^{2-} and two F^{-} ions.

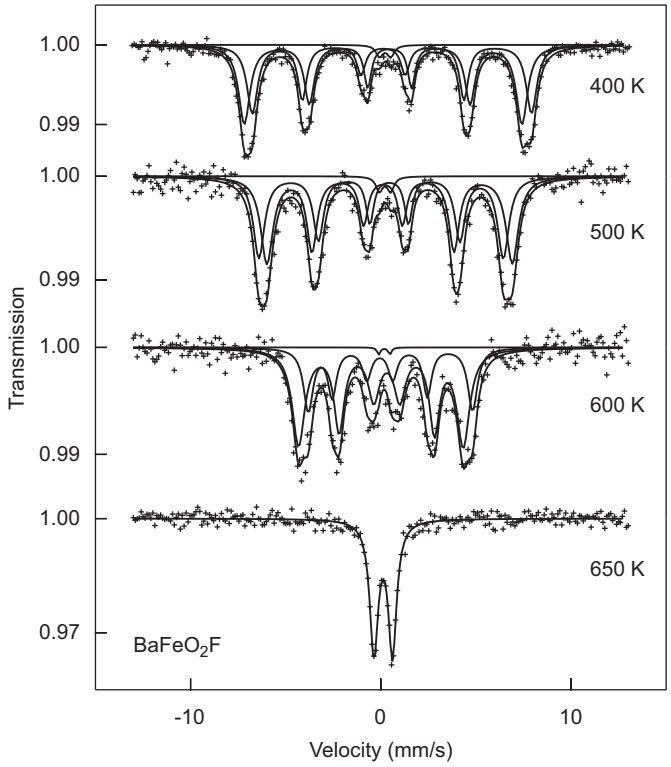

Fig. 5. ^{57}Fe Mössbauer spectra recorded from $BaFeO_2F$ between 400 and 650 K. The spectra were fitted with phenomenological components to measure the magnetic ordering temperature.

hyperfine field at 0 K, T_c is the magnetic ordering temperature and β is usually in the range of 0.25–0.33 and, in this calculation, was taken as 0.3. The results displayed in Fig. 6 show good agreement between the experimentally determined data and those predicted theoretically.

The ^{57}Fe Mössbauer spectra recorded between 10 and 300 K were analysed to test a model for the random occupation by fluorine of anion sites. This model assumes a charge neutral perovskite-related unit cell with four O^{2-} and two F^- anions. Spatially the two F^- anions can be in cis or trans arrange ments with relative frequencies of 4:1 for a purely random occupation in the iron coordination sphere. The principal axes of the electric field gradients (EFG) are taken to be along the directions of maximum symmetry in each case (parallel to the F^- trans direction and along the direction of the bisector of the two F^-anions in the case of the cis arrangement). The hyperfine field is assumed to be parallel to a cube edge as in most antiferromagnetic perovskite-related structures. This model gives rise to four magnetic sextet components—two arising from the cis arrangement with the hyperfine field making angles of 45° and 90° with the EFG in an intensity ratio of 2:1 and two from the trans arrangement with the hyperfine field making angles of 90° and 0° to the EFG with an intensity ratio of 2:1. Thus the fitting area ratios were initially fixed as 8:4:2:1 respectively, with subsequent refinement leading to negligible change in these ratios, confirming the random arrangement. The magnitude of the quadrupole interaction is fixed at the value of 0.96 mm s^{-1} from the doublet measured at 650 K. This magnitude is taken for cis and trans sites but in the magnetically split spectra a choice of sign remains, which was determined by fitting to be positive for cis and negative for trans sites. The angles between the hyperfine field and the quadrupole interaction are specified as above. The variable parameters are isomer shift and hyperfine field values and a representative selection of these parameters is listed in Table 5. The results show that good fits were obtained with this fitting method for temperatures up to ~150 K. Above this temperature a non-magnetic component with relative intensity ~3% is also required. Nevertheless the good fit of the majority magnetic spectrum gives confidence in the model of F^- distribution that gives a charge neutral perovskite-related unit cell, with a random arrangement of F^- anions.

Table 5
Fitting parameters for the ^{57}Fe Mössbauer spectra. The table contains parameters for two different fitting procedures. The spectra from 10 to 300 K were fitted with components with parameters partly determined by a model of the perovskite cell containing four O^{2-} and two F^- ions. The spectra from 400 to 650 K were fitted with phenomenological components to obtain the magnetic ordering temperature. Isomer shift values are quoted relative to metallic iron at 298 K.

Temperature (K)	Isomer shift (mm/s)	Quadrupole interaction (mm/s)	Line width (mm/s)	Hyperfine field (kG)	Relative area (%)
10	0.54	0.24	0.56	550	53.3
	0.53	−0.46	0.56	548	26.7
	0.50	0.48	0.56	522	13.3
	0.41	−0.66	0.56	541	6.7
80	0.55	0.24	0.56	549	53.3
	0.49	−0.46	0.56	545	26.7
	0.50	0.48	0.56	524	13.3
	0.42	−0.96	0.56	521	6.7
150	0.52	0.24	0.54	543	52.3
	0.49	−0.46	0.54	538	26.1
	0.50	0.48	0.54	522	13.1
	0.42	−0.96	0.54	535	6.5
	0.66	1.00	0.56	0	2.0
300	0.40	0.24	0.55	503	51.4
	0.37	−0.46	0.55	501	25.7
	0.50	0.48	0.55	495	12.9
	0.42	−0.96	0.55	499	6.4
	0.40	0.88	0.56	0	3.6
400	0.32	0.01		452	77
	0.37	0.01		479	21
	0.22	0.62		0	2
500	0.27	−0.03		384	54
	0.24	0.01		413	44
	0.17	0.74		0	2
600[a]	0.17	0.01		258	73
	0.23	−0.03		288	27
650	0.13	0.96		0	100

[a] The quadrupole split absorption equated to less than 1% of the spectral area at 600 K.

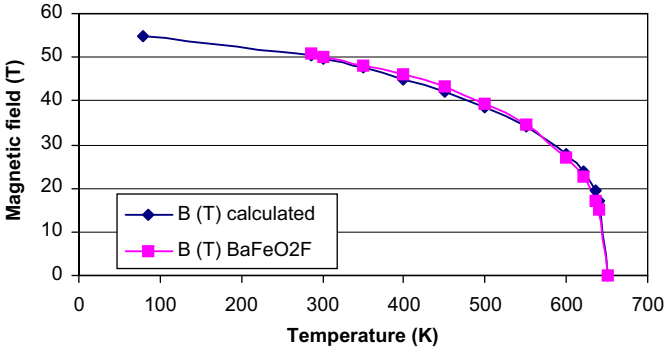

Fig. 6. Variation of the magnetic hyperfine field in $BaFeO_2F$ with temperature. The values of hyperfine field are taken from the spectra shown in Fig. 5.

4. Conclusions

The cubic oxide fluoride $BaFeO_2F$ is substantially different from the related phase of composition $SrFeO_2F$. The main magnetic

features observed here concerning the magnetic properties of $BaFeO_2F$ are

(i) The variation of magnetic hyperfine field with temperature, which establishes a magnetic ordering temperature of $T_N = 645 \pm 5$ K.
(ii) Neutron diffraction measurements down to 5 K, which establish that the Fe^{3+} moments are ordered in a G-type antiferromagnetic structure.
(iii) The magnetisation results that modify the picture of a pure G-type antiferromagnet introducing evidence of a weak ferromagnetic structure with canting of the moments by $\sim 0.16^{\circ}$ to give a weak ferromagnetic moment of $\sim 0.01\ \mu_B$ per Fe^{3+} ion.
(iv) The large mean square displacement of the Fe^{3+} ions down to 5 K in the neutron diffraction data with further refinements suggesting an average 0.25 Å shift off-site.

Acknowledgments

MFT acknowledges EPSRC support for the low temperature Mössbauer spectroscopy. We thank EPSRC for funding (studentship for CH), ISIS, Rutherford Appleton Laboratory for the provision of neutron diffraction beam time, and Ron Smith for the help with the collection of neutron diffraction data and EAM acknowledges The Open University Science Faculty support for the Linux Beowulf cluster.

Appendix. Supplementary materials

Supplementary data associated with this article can be found in the online version at doi:10.1016/j.jssc.2011.04.011.

References

[1] M.G. Francesconi, C. Greaves, Supercond. Sci. Technol. 10 (1997) A29.
[2] C. Greaves, M.G. Francesconi, Curr. Opin. Solid State Mater. Sci. 3 (1998) 132.
[3] E.E. McCabe, C. Greaves, J. Fluorine Chem. 128 (2007) 448.
[4] F.J. Berry, X. Ren, R. Heap, P.R. Slater, M.F. Thomas, Solid State Commun. 134 (2005) 621.
[5] F.J. Berry, R. Heap, O. Helgason, E.A. Moore, S. Shim, P.R. Slater, M.F. Thomas, J. Phys.: Cond. Matter 20 (2008) 215207.
[6] R. Heap, P.R. Slater, F.J. Berry, O. Helgason, A.J. Wright, Solid State Commun. 141 (2007) 476.
[7] P.R. Slater, J. Fluorine Chem. 117 (2002) 43.
[8] A.C. Larson, R.B. Von Dreele, Los Alamos National Laboratory, Report No. LA-UR-96-748, 1987.
[9] O. Helgason, H.P Gunnlaugsson, K. Jonsson, S. Steinthorsson, Hyperfine Interact. 91 (1994) 59.
[10] R. Dovesi, V.R. Saunders, C. Roetti, R. Orlando, C.M. Zieovich-Wilson, F. Pascale, B. Civalleri, K. Doll, N.M. Harrison, L.J. Bush, Ph. D'Arco, M. Llunell, CRYSTAL06 User's Manual, University of Torino, Torino, 2006.
[11] M. Catti, G. Valerio, R. Dovesi, Phys. Rev. B 51 (1995) 7441.
[12] M. Catti, G. Sandrone, G. Valerio, R. Dovesi, J. Phys. Chem. Solids 57 (1996) 1735.
[13] J.M. Ricart, R. Dovesi, C. Roetti, V.R. Saunders, Phys. Rev. B 52 (1995) 2381.
[14] S. Piskunov, E. Helfets, R.I. Eglitis, G. Borstel, Comp. Mat. Sci. 29 (2004) 165.